A Nondestructive Integrity Test for Membrane Filters Based on Air-Coupled Ultrasonic Spectroscopy

Tomás E. Gómez Álvarez-Arenas

***Abstract*—This work describes the application of an ultrasonic air-coupled characterization technique to membrane filters. Coefficient of transmission of sound at normal incidence through each membrane in the frequency range 0.55 MHz–2.4 MHz was measured. For all cases, at least one thickness resonance was observed. From these measurements density, velocity, and attenuation of ultrasonic longitudinal waves are calculated and compared to available filtration data such as water flux measurements and bubble point data, both provided by manufacturers. Results show that velocity of ultrasonic waves in membrane filters depends on the membrane grade and can be correlated to filtration properties; attenuation per wavelength is independent of membrane grade but sensitive to moisture content. Advantages of this technique over other conventional membrane tests are pointed out.**

I. Introduction

Sterilizing filtration can be defined as the process of removing all microorganisms, excluding viruses, from a fluid stream [1]. Toward this end, microporous membrane filters have been used successfully for many years. A fundamental element of sterility assurance is the integrity testing of sterilizing-grade filters before and after use. This physical integrity test determines that the filter is undamaged and is similar to those filters validated by the manufacturer when establishing integrity test specifications for that given filter. Therefore, an integrity test is not an intrinsic determination of the properties of the filter but just an indirect measurement of some parameters that can be correlated to the specific criteria the filter must meet.

The most stringent integrity test for a sterilizing grade membrane is a bacterial retention test. Unfortunately, this is a destructive test. It is of much interest to have a nondestructive integrity test, which should be easy to perform in a reproducible manner, and with results that could be correlated to the production of sterile effluent in a bacterial challenge test [2]. The objective of such a test also could be defined as determining "the presence of oversized pores or defects which compromise a given filter's retention capability without destroying the filter [1];" their results must be able to predict the performance of the filter for the particular application it is intended for and under realistic operation conditions. Integrity testing, performed before use, monitors filter integrity prior to processing to prevent the use of nonintegral filter. Integrity testing, performed after use, can detect if the integrity of the filter has been compromised during the process. There are several types of nondestructive integrity tests: bubble point test, diffusion test, and water-flow integrity test. Other tests such as the pressure hold, forward flow, and pressure decay tests are variations of the diffusion test. The forward or diffusive flow test cannot be performed on a small area disk because the fluid flow is too low to measure accurately with current instrumentation. This has led some authors to suggest that only a bubble point-type test, which can be performed both on small-area disks and larger-area filter assemblies, can be used for integrity testing of sterilizing-grade filters [2]. The most widely used nondestructive integrity test, the bubble point test, is based on the fact that liquid is held in the pores of the filter by surface tension and capillary forces. The minimum pressure required to force liquid out of the pores is a measure of the pore diameter.

Nevertheless, results from bubble point tests depend on filter area, method used, and whether it is manual or automatic. Some authors [2]–[4] have shown differences up to 20% in bubble point values measured for the same filter but by different equipments.

It is well-known that velocity and attenuation of sound in porous materials are closely related to parameters such as pore size, porosity, tortuousity, permeability, and flux resistivity. For example, flux resistivity has been related to the attenuation of sound waves (acoustic absorbents) [5], [6]. For some other porous materials, velocity of slow longitudinal sound waves has been related to pore tortuosity, diffusion, and transport properties [7]–[11]. Attenuation of sound is very sensitive to the appearance of any external agent in the pore space (e.g., moisture) [12], [13] and has been used to monitor wetting and drying processes [14]. Velocity of ultrasonic waves has been used in the past to measure elastic coefficients of different kinds of paper and correlate them with properties such as tensile breaking strength, compressive strength, etc. [15]–[19]. Although all these results are encouraging, there is no study about the acoustics of membrane filters and the relationship between acoustic and filtration properties.

Materials characterization by ultrasonic waves uses, commonly, water as a coupling medium between transducers and samples. However, water may cause permanent

Manuscript received July 15, 2002; accepted December 31, 2002.

The author is with the Departamento de Señales, Sistemas y Tecnologías Ultrasónicas. Instituto de Acústica, C.S.I.C., 28002 Madrid, Spain. (e-mail: tgomez@ia.cetef.csic.es).

0885–3010/$10.00 © 2003 IEEE

damage or undesired contamination to many porous materials; for some cases, dry coupling is not a solution for contact and may damage the weak porous structure of the material, for such cases noncontact ultrasonic inspection techniques should be used.

Over the last 30 years, there have been significant advances in the field of air-coupled transducers, the availability of such transducers has enabled the development of many different applications (nondestructive evaluation (NDE), surface inspections, materials characterization, etc.). An excellent review about the development and applications of air-coupled sensors, noncontact transducers, and transducers for NDE is given [20]–[22]. Concerning piezoelectric transducers, a significant advance is related to the availability of better materials and methods for impedance matching [23]–[25].

Concerning materials characterization, air-coupled ultrasound has been applied to different cases. Paper has been characterized using plate wave resonances: Luukkala *et al.* [15] measured the velocity of the Ao and So Lamb modes in thick cardboard (0.4–0.85 mm) samples in the frequency range 60–350 kHz; Habeger *et al.* [16] obtained similar results for chipboard samples (0.75 mm) in the frequency range 100–400 kHz; Khoury *et al.* [17] measured the velocity of the Ao mode in packing paper (0.27 mm) for the frequency range (200–500 kHz) and derived the Young modulus. Thickness resonances also have been used to characterize paper: McIntyre *et al.* [19] measured longitudinal velocity in thick paper samples (>0.2 mm) for the frequency range 0.1–1 MHz and estimated moisture and glue content, Gómez Álvarez-Arenas *et al.* [26] measured thickness and plate resonances in thinner paper samples (0.1–0.15 mm) in the frequency range 0.5–1.2 MHz. Polymers also have been studied: Luukkala *et al.* [15] show measurements of PVC sheets using plate wave resonances at 200 kHz, Schindel and Hutchins [27] measured time-of-flight and thickness resonances to get longitudinal velocity for several polymer and composite plates, Anderson *et al.* [28] obtained elastic constants of reinforced graphite fiber polymer and composites plates from velocity measurements of the Ao Lamb mode (100–200 kHz). Hutchins *et al.* [29] excited both thickness and plate resonances in Plexiglass and carbon fiber-reinforced composite plates, but no material property was obtained. Safaeinili *et al.* [30] obtained complex velocities (longitudinal and shear waves) in composite laminates from measurement of plate wave resonances (0.4–1.1 MHz). Metals have been studied using Lamb waves by Luukkala and Meriläiner [31] (Ao mode for aluminium and copper plates, frequency range 70 kHz-100 kHz) and using thickness resonances at normal incidence by Wright and Hutchins [32] (0.4–1.1 MHz), although no information about the material was derived. Wood has been studied by means of thickness resonances and through transmission at oblique incidence: Fortunko *et al.* [33] measured through transmitted air-coupled signals in balsa wood samples, Schindel and Hutchins [27] measured velocity of longitudinal waves in different types of woods. Air-coupled ultrasound, through transmission and low frequency, have been used to transmit ultrasonic signals through many different samples with different purposes: for the measurement of time-of-flight and longitudinal wave velocity in natural rocks [10] and plastic foams (60–420 kHz) [34], for the measurement of the longitudinal wave velocity and calculation of the permeability of fabrics (20–60 kHz) [35], for the measurement of shear modulus and Poisson coefficient of open-bubble foams (10–150 kHz) [36], and for the study of attenuation in high porosity foams (50–800 kHz) [37]. Aerogels also have been studied: thickness resonances in the frequency range 4–15 kHz were used by Armand and Guyomar [38], and a comprehensive viscoelastic characterization (i.e., velocity and attenuation and their variation with the frequency for longitudinal and shear waves) has been obtained using thickness resonances at normal and oblique incidence (0.4–1.3 MHz) [39].

In this paper an air-coupled ultrasonic technique is used for the measurement of the acoustic properties of filtration membranes. The objective is to determine the possibility to develop an ultrasonic nondestructive integrity test. A wide set of commercial membranes is studied and correlations between acoustical measurements and filtration properties are sought. Membranes are highly porous (>70%) and thin sheets (90–150 μm) materials. They exhibit low figures for the acoustic impedance (0.07–0.3 Mrayl) and the velocity of sound propagation (200–600 m/s). Accurate measurements of velocity, attenuation, and density of the membrane can be obtained from the analysis of thickness resonances of these samples in the frequency domain. The observation of the first thickness resonance of the membranes makes it necessary to work at higher frequencies than done before, for most of the membranes exhibit its first thickness resonance close to 2 MHz.

II. Theoretical Background

The technique is based on the spectral analysis of broadband ultrasonic pulses transmitted through the samples and the solution of the so-called inverse problem [40]. This is a very well-known technique that has already been used for water immersion measurements [41], [42]. In this case, an airborne ultrasonic pulse is set to impinge normally on membrane filters surface; through transmitted signal is received and analyzed. Toward this end, the frequency spectrum of the ultrasonic pulse incident on the filter membrane must contain, at least, one eigenfrequency (thickness mode) of the sample.

Theoretical modeling of the problem of the transmission of ultrasonic waves through a plate separating two media (1 and 3) is carried out considering plane longitudinal waves, normal incidence, and a one-dimensional model. Displacement vector potential can be written in the three space regions (m) denoted as (1: medium 1, 2: membrane, 3: medium 3) [43]:

$$\varphi_m = \varphi_m^1 \exp\left[ik_m z\right] + \varphi_m^2 \exp\left[-ik_m z\right], \quad m = 1, 2, 3, \tag{1}$$

where k_m is the wavenumber in each region of the space, and t is the thickness of the membrane. Faces of the membrane are located at $z = 0$ and $z = t$.

Displacement vector u is calculated from the scalar potential φ by:

$$u_m = grad\varphi_m. \tag{2}$$

Stress (σ) is calculated from the constitutive equations in each region of the space:

$$\sigma_z^m = c_z^m \frac{\partial u_z^m}{\partial z},\ \mathrm{m} = 1, 2, 3, \tag{3}$$

where c_z^m are the elastic constant for the z direction of each space region m.

Stress and displacement must be continuous across membrane surfaces ($z = 0$, $z = t$). These boundary conditions along with (1)–(3) provide a linear system of four equations that can be analytically solved for the coefficients φ_m^i. From these coefficients, displacements, stress, and energy flux in any point of the space can be derived. The transmission coefficient (T) is defined as the ratio of transmitted to incident energy fluxes; a simple analytical expression is obtained:

$$T = \frac{4Z_3\left(Z_2Z_3\right)^2}{\left[\left(Z_1Z_2 + Z_3Z_2\right)^2\cos^2\widetilde{k}_l t + \left(Z_2^2 + Z_1Z_3\right)^2\sin^2\widetilde{k}_l t\right]}, \tag{4}$$

where t is the thickness of the membrane, $\widetilde{k}_l$ is the complex wave vector in the membrane defined as $\widetilde{k}_l = k_l - i\alpha_l = \omega/c_l - i\alpha_l$, where k_l is the wave vector, α_l is the longitudinal wave attenuation, c_l is the longitudinal phase-velocity, and ω is the angular frequency. Z is the specific acoustic impedance, defined as: $Z = c_l\rho$, where ρ is the density, the subindex 1, 2, and 3 refers to media 1, membrane filter, and 3, respectively. When 1 and 3 have the same acoustic impedance, T is given by:

$$T = \frac{4}{2 + 2\cos^2\widetilde{k}_l t + \dfrac{Z_2^4 + Z_1^4}{Z_2^2Z_1^2}\sin^2\widetilde{k}_l t}. \tag{5}$$

Attenuation is introduced by the viscoelastic correspondence principle [44].

From the experimental T versus frequency graph, a first approach to velocity and attenuation of longitudinal waves in membranes and density of the membranes are obtained as follows:

Calculation of the velocity of sound in the membrane:

Maximum values of T are located at: $kt = n\pi$, n = $0, 1, 2\ldots$. Therefore:

$$f^{(n)} = nc_l/2t. \tag{6}$$

The thickness of the membrane (t) is independently measured and the resonant frequency $\left(f^{(n)}\right)$ is measured from the T vs. frequency graph. The velocity of sound in the membrane is calculated from (6).

Calculation of the density of the membrane:

Minimum values of T are located at $kt = \frac{1}{2}n\pi$, n = $1, 2, \ldots$. From (5) minimum value of T is given by:

$$T_{\min} = \frac{4Z_2^2Z_1^2}{\left(Z_2^2 + Z_1^2\right)^2}. \tag{7}$$

Calculation of the attenuation of sound in the membrane.

Q-factor of the resonance is defined as:

$$Q = \frac{f_r}{\Delta f}, \tag{8}$$

where Δf is the width of the resonance peak (T) measured at half-maximum value.

Total loss of energy inside the membrane, at resonance, can be calculated from the damping of the resonance peak. It is given by [45], [46]:

$$\widetilde{\alpha} = \frac{\pi f_r}{c_l Q}. \tag{9}$$

To obtain the attenuation of sound waves in the membrane (α), it is necessary to consider that total loss ($\widetilde{\alpha}$) measured from the damping of the resonance peak has two contributions: the first due to the intrinsic attenuation in the material and the second due to radiation of sound from the membrane to the surrounding space.

Considering the reflection coefficient at a single membrane/air interface (R) that is defined as:

$$R = \frac{\left(Z_2 - Z_1\right)^2}{\left(Z_2 + Z_1\right)^2}. \tag{10}$$

Attenuation in the material can be obtained from the following expression:

$$\alpha = \widetilde{\alpha} + \frac{\log R^2}{2t}. \tag{11}$$

These values of velocity, density, and attenuation are entered on a fitting routine to find the values that provide the best agreement (in the sense of least squares) between experimental measurements of T and theoretical results from (5). The fitting routine operates as follows. First, density and attenuation are kept equal to values obtained from (7) and (11), and velocity is recalculated; only slight differences between the values obtained from this curve fitting and from (6) are obtained. Then density is changed, but velocity and attenuation are kept constant to find out the value that provides the best fitting between theoretical and experimental results. The same procedure is applied to the attenuation. These two steps (density and attenuation calculations) are consecutively repeated until the best agreement between theoretical curve and experimental values is obtained.

When samples under test have high acoustic impedance values, accurate measurement of the minimum of T cannot be achieved because of a very low SNR at this point. In

such cases, density cannot be calculated from resonance curves and must be measured by an independent method. For membrane filters, acoustic impedance is not very high and minimum value of T, and therefore density, can be measured.

The most important restriction to this method is given by the requirement that samples must be completely flat and homogeneous, and surfaces parallel (uniform thickness). Any departure from this ideal situation introduces an extra loss in the thickness resonances of the sample; calculated attenuation is overvalued. For the same reason, density and elastic constants also must be uniform. Filter membranes do meet these requirements and only for wetted membranes some of these problems may be observed.

In some other cases, the hypothesis of plane wave must be replaced by a more realistic representation of the acoustic beam. This is especially important for oblique incidence and has previously been studied for solid plates in a liquid [47], [48] and in air [49]. Even beam effects should be considered for normal incidence when distance between the sample and the emitter is big enough to have significant diffraction effects. Recently, Temsamani *et al.* [50] studied this effect. The analysis is based on the correction introduced by Bass:

$$(P)_{Av} \approx \frac{\rho v \omega}{k} \exp(-ikz) \left(1 - \left(1 - \frac{\zeta^2}{2k^2a^2}\right)(J_0(\zeta) + iJ_1(\zeta)) \exp(-i\zeta) - \frac{\zeta^2}{k^2a^2}(iJ_1(\zeta)/\zeta) \exp(-i\zeta)\right), \quad (12)$$

where $\zeta = \frac{k}{2}\left(\left(z^2 + 4a^2\right)^{\frac{1}{2}} - z\right)$ and ρ is the density, v is the velocity, a is the radius of the (circular) transducer, ω is the angular frequency, k is the propagation constant, and z is the distance from the transducer surface. In this work, experimental working conditions are so established that diffraction effects can be neglected and, therefore, at normal incidence, the hypothesis of the plane wave is assumed.

Filter membranes are open-pore porous materials. Analysis given in this section assumes that wavelength is much more larger than pore dimensions and, therefore, considers that the material is homogeneous. A more refined approach is given by the Biot's theory [52], [53]. This theoretical approach describes the propagation of acoustic waves in fluid-saturated porous media taking into account the interaction between the fluid space and the solid space. A fundamental prediction is the appearance of two different longitudinal modes. Transmission through porous plates using Biot's theory has been studied by many authors [54]–[56]. In this work, however, no evidence of the appearance of these two longitudinal modes is observed, so the theoretical analysis may be reduced to the study of a homogeneous effective medium whose properties are the same as those of the real porous medium. Nevertheless, use of concepts from Biot's theory is useful to qualitatively explain the behavior of acoustic waves in some of the cases presented here.

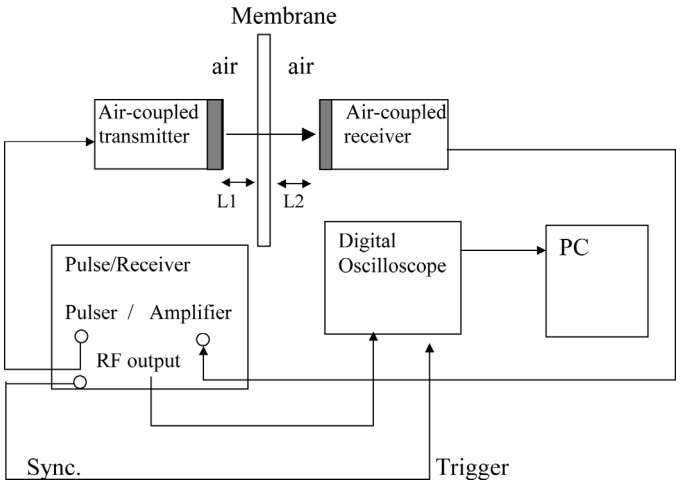

Fig. 1. Experimental set-up.

III. Experimental Set-up

For the experimental work, two pairs of especially designed air-coupled piezoelectric transducers were used [26], [57], [58]. Center frequency is 1 MHz and 1.7 MHz and usable frequency band is 0.55–1.3 MHz and 1.3–2.4 MHz, respectively; the diameter of the active area is 25 mm. Matching to the air is achieved by a stack of two quarter wavelength matching layers.

Fig. 1 shows the scheme of the experimental set-up. The two transducers are positioned facing each other. Transmitter transducer is driven by a high-voltage square pulse. It launches an ultrasonic pulse to the air that is picked up and converted into electric voltage by the receiver transducer; it is amplified, digitized by an oscilloscope (Tektronix 2432 A, Tektronix Holland, NV, The Netherlands), stored on a floppy disk (Tektronix 2402A, Tektronix, Inc., Beaverton, OR) and transferred to a computer. First, received signal through the airgap without any membrane in between is digitized by the oscilloscope and transferred to the computer; its frequency spectrum is calculated (fast Fourier transform or FFT). Then the membrane is put in between the transducers, parallel to transducers faces; the received signal is again recorded and FFT calculated. Transfer function for the membrane (TF) is defined as $TF = \left(A_{\text{sample}}/A_{\text{ref}}\right)$ where A_{sample} and A_{ref} are the amplitudes of the FFT of recorded waves with and without membrane in between the transducers, respectively. In this case: $A^2_{\text{sample}}/A^2_{\text{ref}} = T$ [59].

In order to simplify signal processing, distances between transducers and sample (L1 and L2) should be long enough so that overlap between the direct signal (first arrival corresponding to transmission through airgap/sample/airgap) and multiple reverberations between transducers and sample surfaces are avoided. Longest observed signals (transmitted through a membrane) in the

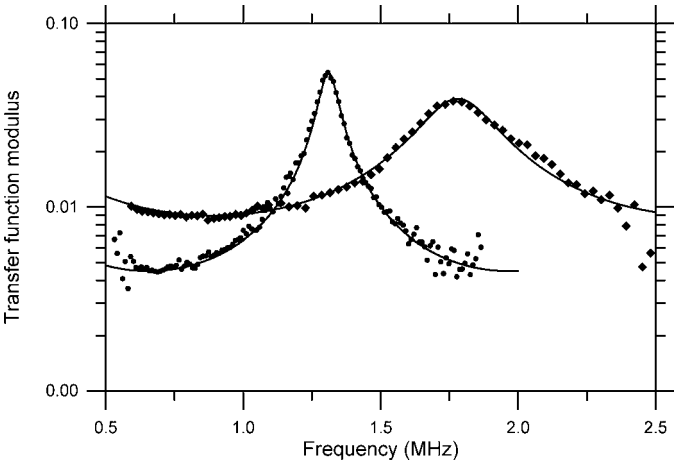

Fig. 2. Modulus of the transfer function. Polypropylene filter membrane (♦) and a cellulose ester membrane (•). Solid line is theoretical calculations from (5).

time domain were about 30 μs. Velocity of sound in air is approximately 340 m/s, then L1 and L2 should be longer than 6 mm. It is interesting to point out that, because of the resonance in the membrane, transmitted signal through the airgap/sample/airgap is much longer in the time domain than the transmitted signal through the airgap without the sample in between. Nevertheless the duration of this signal is much shorter than those observed for other solid samples such as metals or polymers; this is due to the much lower value of the acoustic impedance of filters compared to any solid material and much higher attenuation.

A second restriction to impose is that L1 has to be short enough so that diffraction of the sound beam when it reaches the surface of the sample could be neglected. Most of the observed thickness resonant frequencies are in the range 1–2.2 MHz, although a few of them appear at lower frequencies; the lowest resonant frequency corresponds to some wetted filters (0.65 MHz). From (12) and considering a frequency of 0.55 MHz, maximum diffraction correction to the pressure can be maintained below 5% if the distance between transmitter and sample is kept under 8 mm.

A distance L1 about 7 mm was used in experimental set-up. As samples are very thin (<150 μm) and velocity in the samples very low, diffraction within the samples also is neglected. Apart from having a clear signal and a good SNR, there is no restriction on the maximum length of L2. As L2 is increased, amplitude of received signal decreases because of diffraction and attenuation in the air gap; typical values of L2 were in the range 1–4 cm.

Fig. 2 shows modulus of the transfer function versus frequency for two different membranes: a polypropylene membrane and a cellulose ester membrane. From Fig. 2 we obtain: $f_{\rm res} = 1.78$ MHz, $Q = 6.57$, and $|T_{\rm min}| = 7.5\times10^{-5}$ for the polypropylene membrane and $f_{\rm res} = 1.31$ MHz, $Q = 16$, and $|T_{\rm min}| = 2.025 \times 10^{-5}$ for the cellulose ester membrane. From these data and (6), (7), and (11), it is calculated: $v = 365$ m/s, $\rho = 258$ kg/m^3, and $\alpha = 2155$ Np/m for the polypropylene membrane and $v = 393$ m/s, $\rho = 461$ kg/m^3, $\alpha = 578$ Np/m for the cellulose membrane.

Fitting the theoretical curve given (5) to the experimental measurements, we obtain: $v = 365$ m/s, $\rho = 240$ kg/m^3, and $\alpha = 2200$ Np/m, for the polypropylene membrane and $v = 393$ m/s, $\rho = 461$ kg/m^3, $\alpha = 530$ Np/m for the cellulose membrane. These are the values used to compute the theoretical curves also shown in Fig. 2.

The main source of error in the determination of the velocity comes from the measurement of the thickness of the sample, which is about 5%. The second source of error comes from the determination of the resonant frequency; this is related to the sampling rate and total length of the signal in the time domain. The length of digitized signals was 1024 points. When needed, signals were padded with zeros, discretization of the signal in the frequency domain is about 5 kHz, then a typical uncertainty about 5% and 4% for the determination of the velocity and the Q-factor, respectively, is obtained. The accuracy in the determination of the density depends on the value of the acoustic impedance of the membrane; the higher the impedance the lower the accuracy. The curve-fitting procedure leads to determination of the density with a typical sensitivity of ±25 kg/m^3. An uncertainty about 10% for the attenuation is produced.

IV. Materials

Table I summarizes the main properties of the studied membrane filters. Different materials and different grades of the same material are analyzed. Two magnitudes to characterize the filtration properties of each membrane also are provided: water flux and bubble point. Water flux is measured at 0.7 bar of pressure gradient across the membrane (it is normally given in mL/min/cm^2). Bubble point is commonly used to characterize membrane filters and monitor product consistency and quality; it is one of the most used integrity tests for membrane filters. The bubble point itself is a determination of the minimum pressure at which a wetting liquid is pressed out of the pore system of a membrane while forming a steady bubble chain. In other words, the pressure that can overcome the capillary action of the fluid within the pore (the largest pore). The bubble point is then given by:

$$BP = \frac{4\kappa\sigma\cos\Theta}{d}, \tag{13}$$

where BP is the bubble point, σ is the surface tension, κ is a shape correction factor, Θ is the solid-liquid contact angle and d is the diameter of the pore.

From (13) it is clear that the larger the pore size the lower the bubble point. Lowest bubble point values in this work correspond to cellulose membranes (about 0.4 bar) for pore size about 5 μm. It also is observed for different grades of the same material that the changes in the microstructure of the membrane that give rise to a larger

TABLE I
MAIN PROPERTIES OF THE EMPLOYED MEMBRANES AND OBTAINED ACOUSTIC PROPERTIES.

Material	Water flux @ 0.7 bar (mL/min/cm^2)	Bubble point (bar)	Velocity (m/s)	Attenuation per wavelength (Np)
PVDF	9.6	1.1	515	0.322
Nylon	8	3.8	850	0.453
Polypropylene	28	1.38	363	0.531
Polypropylene	17	2.9	377	0.439
Polyetersulfone	5	6.9	660	0.124
Polyetersulfone	22	3.2	435	0.120
Polyetersulfone	44	2.1	374	0.132
Cellulose ester	0.15	21.1	910	0.200
Cellulose ester	1.5	14.1	650	0.229
Cellulose ester	18	3.52	404	0.202
Cellulose ester	60	2.11	281	0.216
Cellulose ester	190	1.2	237	0.212
Cellulose ester	270	0.77	222	0.241
Cellulose ester	320	0.7	242	0.205
Cellulose ester	580	0.42	226	0.249

pore size also produce a higher porosity, a lower density, and a softer membrane.

V. Experimental Results and Discussion

The main goal of this work is to show that acoustic and filtration properties are closely correlated so that classical integrity tests can be replaced by the measurement of the acoustic properties. A discussion on how the presence of elements that may compromise filter integrity affects the acoustic properties of the membrane also is included. In particular, the influence of moisture in the membrane is analyzed.

A. Relationship Between Acoustical and Filtration Properties

Measured acoustic properties for each membrane along with filtration properties and material description are collected in Table I. Fig. 3 shows a comparison between the density obtained from weighing the sample and from the ultrasonic method; agreement between both measurements is within experimental error range. Density measurements could be used to determine porosity.

Fig. 4 shows the plot of the measured velocity of ultrasonic waves versus bubble point. A linear relationship between velocity and bubble point is observed. At very low bubble point values velocity of ultrasonic waves in membranes approaches to a nonzero lower bound (v_o), which is lower than the velocity of ultrasonic waves in air. Two different simplifications of Biot's theory give rise to such a lower bound (see, for instance, [55] and [60]) both for the high frequency limit, both provide a velocity:

$$v_0 = \frac{v}{\sqrt{\alpha}}, \tag{14}$$

where α is the tortuosity of the pores and v_f is the velocity of sound in the fluid. High frequency limit of Biot's

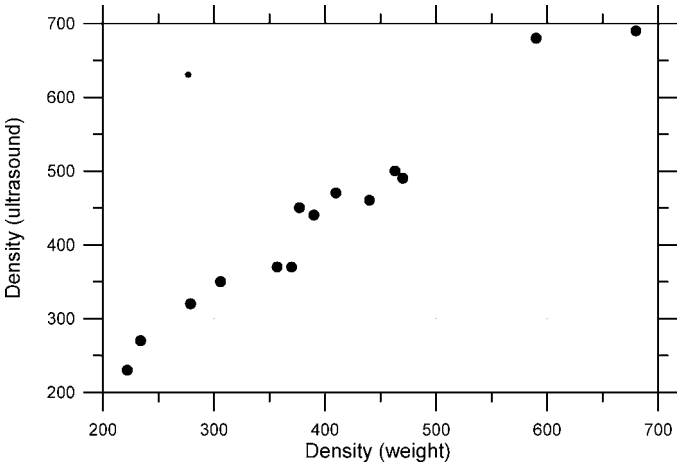

Fig. 3. Comparison between density obtained from the through thickness membrane resonance and from weighing samples having a known volume.

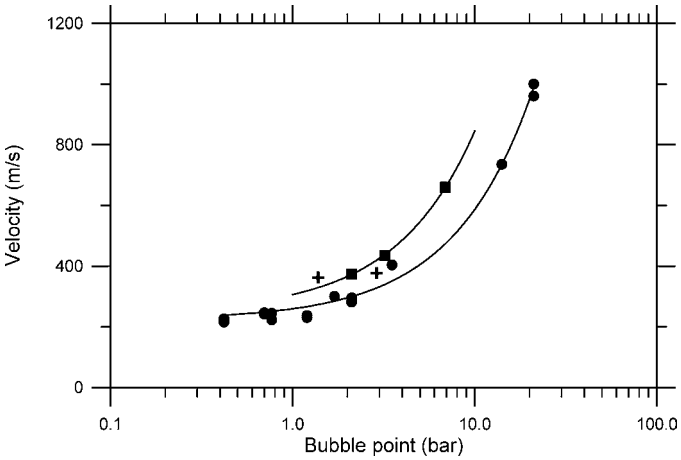

Fig. 4. Velocity of ultrasonic waves vs. bubble point: (■), polyetersulfone membranes; (●), cellulose ester membranes; (+), polypropylene membranes. Solid line, linear fitting (16) for polyetersulfone and cellulose ester membranes.

theory is obtained when the viscous skin depth is smaller than pore size. Within this approximation, vibrations in the solid and the fluid are not coupled by viscous forces. The crossover between the high-frequency and the low-frequency approximations is located at:

$$f_c = \frac{\eta}{\rho_f \pi a^2}, \tag{15}$$

where η is the fluid viscosity, ρ_f is the fluid density, and a is the pore size. A velocity such as that of (14) correspond to a wave propagation that takes place mainly in the fluid phase; its velocity is lower than velocity in the fluid because of the tortuosity of the pores. Lower values of bubble point correspond to membranes having a pore size of a few microns and, therefore, a value of f_c of about 200 kHz.

The first simplification of Biot's theory providing a limit for the velocity such as that of (14) is obtained when the pore fluid is much more compressible than the solid frame [8], [10], [60]. Velocity v_o correspond to a Biot's longitudinal slow wave. The second is obtained for very weak porous frames (in the unconsolidated limit the velocity of the slow longitudinal wave is zero) and density and elastic moduli of the solid much higher than density and elastic moduli of the fluid [55], [60]. In this case, velocity v_o corresponds to a Biot's longitudinal fast wave.

If the first interpretation is considered (v_o correspond to a slow wave), then a transition from slow wave to fast wave propagation should be observed when membranes having higher bubble point values are studied. So far, there is no clear evidence of such a transition (discontinuity in the velocity or change in the attenuation). This could be avoided if the second interpretation given is considered (v_o corresponds to a fast wave). The problem in this case comes from the assumed hypothesis that the frame is very weak (unconsolidated), which may appear unsuitable for membrane filters.

Comparing membranes of the same material but of different grades, it is observed that those having a higher bubble point value also have a smaller pore size, a lower porosity, and higher bulk modulus of the porous frame. The actual way these later properties are related to the former one is very complex and depends on the solid material used to produce the membrane and the manufacturing route. All these changes can be accounted for by a simple empirical linear relation between ultrasonic velocity and bubble point for different grades of the same material:

$$\frac{v - v_0}{v_0} = k \cdot BP, \tag{16}$$

where BP is the bubble point expressed in bar, k is a constant that depends on the material, v is the ultrasonic velocity in the membrane in meters per second and v_0 is, as seen above, a constant equal to the lowest value of the velocity of ultrasonic waves in the material, this corresponds to the grade having the lowest bubble point value and depends only on pore tortuosity and velocity in the fluid (air in this case). Solid lines in Fig. 4 correspond to cellulose ester membranes $k = 0.16$ bar^{-1} and $v_0 = 222$ m/s and for polyetersulfone membranes $k = 0.24$ bar^{-1} and $v_0 = 246$ m/s. These values of v_0 can be used to calculate pore tortuosity from (14).

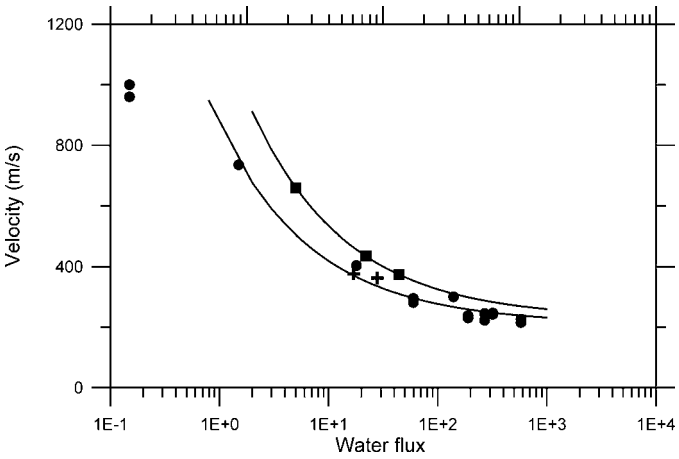

Fig. 5. Velocity of ultrasonic waves vs. water flux (mL/min/cm^2) (▪), polyetersulfone membranes; (•), cellulose ester membranes; (+), polypropylene membranes. Solid line (18) for polyetersulfone and cellulose ester membranes.

Water flux is inversally proportional to flux resistivity. From Biot's theory, it is known that flux resistivity is inversally proportional to the second power of the pore size [52], [53]. From this and (13), we derive a relationship between bubble point (BP) and water flow (WF):

$$BP \propto \sqrt{\frac{1}{WF}}. \tag{17}$$

Therefore, (16) and (17) leads to:

$$\frac{v - v_0}{v_0} \propto \sqrt{\frac{1}{WF}}. \tag{18}$$

Fig. 5 shows the graph of velocity versus water flux. The WF is the water flux in mL/min/cm^2 measured at 0.7 bar. Fittings following (18) for polyetersulfone and cellulose filters also are shown; obtained values of v_0 are 229 m/s and 211 m/s, respectively, which are in good agreement with those results obtained from fitting (16) to experimental data in Fig. 4.

Calculated attenuation per wavelength also is shown in Table I. It is constant for each material regardless of membrane grade. Mean values of attenuation per wavelength and observed variation between different grades are: polyetersulfone: 0.125 Np (4.8%); cellulose ester: 0.219 Np (9%); polypropylene: 0.485 Np (8%). In addition, attenuation is very sensitive to membrane fouling, wetting, or damage; therefore, it can be used to determine the status of a membrane regardless of the grade.

B. Membrane Filters With Moisture

The influence of moisture content on the acoustic properties of the membrane also has been studied. Moisture

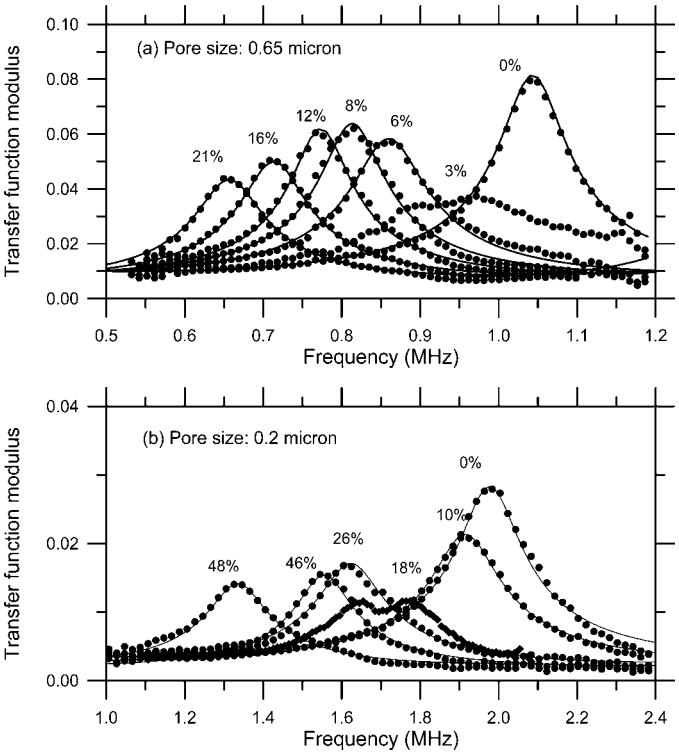

Fig. 6. Modulus of the transfer functionfor two cellulose nitrate membranes at different moisture content as labeled on the graphs. a) Pore size: 0.65 μm, b) Pore size: 0.2 μm. Dots, experimental measurements; solid lines, theoretical calculations.

TABLE II
ACOUSTIC PROPERTIES OF A CELLULOSE NITRATE (PORE SIZE 0.65 μM) AT DIFFERENT MOISTURE CONTENTS.

Velocity (m/s)	Density (kg/m^3)	Attenuation per wavelength (Np)	Volumetric moisture content (%)
197	470	0.385	21
214	420	0.347	16
231	380	0.279	12
244	340	0.290	8
258	320	0.319	6
312	260	0.215	0 (dry)

TABLE III
ACOUSTIC PROPERTIES OF A CELLULOSE NITRATE (PORE SIZE 0.2 μM) AT DIFFERENT MOISTURE CONTENTS.

Velocity (m/s)	Density (kg/m^3)	Attenuation per wavelength (Np)	Volumetric moisture content (%)
347	930	0.355	48
404	910	0.284	46
422	710	0.317	26
497	550	0.275	10
514	450	0.243	0 (dry)

often is present; therefore, it is interesting to determine how much it influences acoustic measurements. In addition, moisture also may be used to simulate membrane fouling and membrane inhomogeneity.

A filter membrane is fully characterized as done before and then it is wetted up to 100% of moisture content. It then is placed in between the transducers (see Fig. 1) and let dry at ambient conditions; transmitted signal is acquired at intervals of 1 minute; the total process last for about 1 hour. The two limits (100% and 0% of moisture content) are granted by weighing the sample. Moisture content at any time in between these two limits is calculated from the density estimated from the measured coefficient of transmission.

Fig. 6 shows the measured modulus of the transfer function for two cellulose nitrate membranes measured at different conditions. The first thickness resonance of the membrane is clearly appreciated in all cases. Results are collected in Table II and Table III.

As the moisture content increases, velocity decreases and attenuation increases. For some cases, it can be assumed that elastic constants of the membrane are not changed by the presence of moisture. Variation of the velocity may be accounted for, in these cases, by the increase of membrane effective density due to the presence of moisture in the pores by: $v = \sqrt{\dfrac{v_{\mathrm{dry}}^2 \rho_{\mathrm{dry}}}{\rho_{\mathrm{dry}} + \phi \rho_{\mathrm{water}}}}$ where subscript dry is used for the properties of the dry membrane and ϕ is the volumetric concentration of moisture (water) in the membrane. This expression explains the observed changes of velocity in Table III, but, it departs from experimental data as moisture increases for the case shown in Table II. In this case, the resonance curve does not fully recover the initial shape after complete drying, which suggest that, in this case, elastic constants of the softer membrane are affected by moisture content.

At a very low moisture content (just before complete drying) the thickness resonance is strongly attenuated and distorted. Because of surface tension, when the moisture content is very low, the continuous water film wetting the membrane breaks down; then moisture in the membrane presents a patchy pattern, which leads to a nonuniform plate that may explain the experimentally observed behavior.

If velocity measurements are going to be used as an integrity test, the change of the velocity due to the presence of moisture may appear misleading, as a lower velocity of sound has been related (see Fig. 6) to a lower bubble point. Nevertheless, attenuation per wavelength, which was observed to be constant and independent of membrane grade (Table I), is strongly dependent on moisture content as shown in Tables II and III. Therefore, the increase of the attenuation can be used to determine whether measured values of the velocity of ultrasonic in a membrane filter are to be explained as the result of the intrinsic properties of the filter or as the result of extrinsic agents: moisture, fouling, etc.

VI. Conclusions

Acoustic properties of several membrane materials and different grades of the same membrane material have been studied. Coefficient of sound transmission at normal incidence, for the frequency range in which the first thickness resonance of the membrane is observed using airborne and wide frequency band ultrasonic pulses has been measured and calculated. Density, velocity, and attenuation of ultrasonic waves in the membrane are ensued from the comparison between measured data and calculated values. Emphasis has been placed on determining a relationship between acoustic and filtration properties; data from standard water flux and bubble point tests provided by the manufacturers have been used. Results show that attenuation per wavelength is independent of membrane grade, and velocity of ultrasonic waves depends on the membrane grade and can be correlated, by means of simple empirical laws, to both bubble point and water flux data.

In addition, to further investigate the possibilities of this technique as a nondestructive integrity test for membrane filters, the influence of the presence of moisture on the acoustic properties of the membrane is studied. Simultaneous measurement of velocity and attenuation of ultrasonic waves in membrane filters can be used to determine both grade and integrity status of a filter membrane and, therefore, used as a nondestructive integrity test.

Results of other integrity tests normally used in the filtration industry depend on a number of variables involved in the test that are not related to the integrity of the filter itself and complicate the interpretation of the results (i.e., fluid used for the test, temperature, seal between membrane and apparatus, etc.); this is not so for the technique shown in this paper, which is simple and fast. In addition, the use of a noncontact technique (air-coupled ultrasound) instead of using water coupling, gel coupling, or dry contact, reduces the handling requirements of the filter membrane extremely and avoids any damage or contamination during the measurements.

Future work will focus on the study of the applicability of Biot's theory to the propagation of acoustic waves in membrane filters and on the determination of the nature of the observed propagation mode. The technique also will be applied to membranes after operation under real operating conditions.

Acknowledgments

The author acknowledges the assistance of Francisco Iglesias (Merck Farma y Química S.A., España) and Luis Quevedo (Pall España S.A.) for providing samples and filtration data. Support by project 07N/0109/2002 funded by CAM is acknowledged.

References

[1] Parenteral Drug Association Technical Report No. 26, "Sterilizing filtration of liquids," *PDA J. Pharm. Sci. Technol.*, vol. 52, no. 3, Supp. 1-31, 1998.

[2] S. Sundaram, J. D. Brantley, G. Howard, Jr., and H. Brandwein, "Consideration in using bubble point type tests as filter integrity tests. Part I," *Pharm. Technol.*, pp. 90–114, Sep. 2000.

[3] S. Sundaram, J. D. Brantley, G. Howard, Jr., and H. Brandwein, "Consideration in using bubble point type tests as filter integrity tests. Part II," *Pharm. Technol.*, pp. 108–136, Oct. 2000.

[4] P. R. Johnston, R. C. Lukaszwicz, and T. H. Meltzer, "Certain imprecisions in the bubble point measurement," *J. Parenteral Sci. Technol.*, vol. 35, no. 1, pp. 36–39, 1981.

[5] M. E. Delany and E. N. Bazley, "Acoustical properties of fibrous absorbent materials," *Appl. Acoust.*, vol. 3, pp. 105–116, 1970.

[6] W. Qunli, "Empirical relations between acoustical properties and flow resistivity of porous plastic open-cell foam," *Appl. Acoust.*, vol. 25, pp. 141–148, 1988.

[7] R. N. Chandler and D. Linton-Johnson, "The equivalence of quasistatic flow in fluid-saturated porous media and the Biot's slow wave in the limit of zero frequency," *J. Appl. Phys.*, vol. 52, no. 5, pp. 3391–3395, May 1981.

[8] D. Linton-Johnson, T. Plona, C. Scala, F. Pasieb, and H. Kojima, "Tortuosity and acoustic slow waves," *Phys. Rev. Lett.*, vol. 49, no. 25, pp. 1840–1844, Dec. 1982.

[9] D. Linton-Johnson, J. Koplik, and L. M. Schwartz, "New pore-size parameter characterizing transport in porous media," *Phys. Rev. Lett.*, vol. 57, no. 20, pp. 2564–2567, Nov. 1986.

[10] P. Nagy, L. Adler, and B. P. Bonner, "Slow wave propagation in air-filled porous materials and in natural rocks," *Appl. Phys. Lett.*, vol. 56, no. 25, pp. 2504–2506, June 1990.

[11] Y. Champoux and J. F. Allard, "Dynamic tortuosity and bulk modulus in air-saturated porous media," *J. Appl. Phys.*, vol. 70, no. 4, pp. 1975–1979, 1991.

[12] B. J. Berger, C. C. Habeger, and B. M. Pankonin, "The influence of moisture and temperature on the ultrasonic viscoelastic properties of cellulose," *J. Pulp Paper Sci.*, vol. 15, no. 5, pp. 170–180, 1989.

[13] T. Schlief, J. Gross, and J. Fricke, "Ultrasonic attenuation in silica aerogels," *J. Non-Cryst. Solids*, vol. 145, pp. 223–226, 1992.

[14] J. Stor-Pellinen, E. Haeggström, and M. Luukkala, "Measurement of paper-wetting processes by ultrasound transmission," *Meas. Sci. Technol.*, vol. 11, pp. 406–411, 2000.

[15] M. Luukkala, P. Heikkila, and J. Surakka, "Plate wave resonance, a contactless test method," *Ultrasonics*, vol. 9, pp. 201–208, 1971.

[16] C. C. Habeger, R. W. Mann, and G. A. Baum, "Ultrasonic plate waves in paper," *Ultrasonics*, pp. 57–79, 1979.

[17] M. Khoury, G. E. Tourtollet, and A. Schröder, "Contactless measurement of the elastic Young's modulus of paper by an ultrasonic technique," *Ultrasonics*, vol. 37, pp. 133–139, 1999.

[18] P. L. Ridgway, A. J. Hunt, M. Quinby-Hunt, and R. E. Russo, "Laser ultrasonics on moving paper," *Ultrasonics*, vol. 37, no. 6, pp. 395–403, 1999.

[19] C. S. McIntyre, D. A. Hutchins, D. R. Billson, and J. Stor-Pellinen, "The use of air-coupled ultrasound to test paper," *IEEE Trans. Ultrason., Ferroelect., Freq. Contr.*, vol. 48, no. 3, pp. 717–727, 2001.

[20] V. Mágori, "Ultrasonic sensors in air," in *Proc. IEEE Ultrason. Symp.*, 1994, pp. 471–481.

[21] D. A. Hutchins and D. W. Schindel, "Advances in non-contact and air-coupled transducers," in *Proc. IEEE Ultrason. Symp.*, 1994, pp. 1245–1254.

[22] W. A. Grandia and C. M. Fortunko, "NDE applications of air-coupled ultrasonic transducers," in *Proc. IEEE Ultrason. Symp.*, 1995, pp. 697–708.

[23] T. E. Gómez, F. Montero, M. Moner-Girona, E. Rodríguez, A. Roig, E. Molins, J. R. Rodríguez, S. Vargas, and M. Esteves, "Low-impedance and low-loss customized materials for air-coupled piezoelectric transducers," in *Proc. IEEE Ultrason. Symp.*, 2001, pp. 1077–1080.

[24] S. P. Kelly, G. Hayward, and T. E. Gómez, "An air-coupled ultrasonic matching layer employing half wavelength cavity resonance," in *Proc. IEEE Ultrason. Symp.*, 2001, pp. 965–968.

[25] M. Toda, "New type of matching layers for air-coupled ultrasonic transducers," *IEEE Trans. Ultrason., Ferroelect., Freq. Contr.*, vol. 49, no. 7, pp. 972–979, 2002.

[26] T. E. Gómez Álvarez-Arenas, B. González, and F. Montero, "Paper characterization by measurement of thickness and plate resonances using air-coupled ultrasound," in *Proc. IEEE Ultrason. Symp.*, 2002, pp. 843–846, to be published.

[27] D. W. Shindel and D. A. Hutchins, "Through-thickness characterization of solids by wideband air-coupled ultrasound," *Ultrasonics*, vol. 33, no. 1, pp. 11–17, 1995.
[28] M. J. Anderson, P. R. Martin, and C. M. Fortunko, "Gas coupled ultrasonic measurement of stiffness moduli of polymer composite plates," in *Proc. IEEE Ultrason. Symp.*, 1994, pp. 1255–1259.
[29] D. A. Hutchins, W. M. D. Wright, and D. W. Shindel, "Ultrasonic measurements in polymeric materials using air-coupled capacitance transducers," *J. Acoust. Soc. Amer.*, vol. 96, no. 3, pp. 1634–1642, 1994.
[30] A. Safaeinili, O. I. Lobkis, and D. E. Chimenti, "Air-coupled ultrasonic estimation of viscoelastic stiffnesses in plates," *IEEE Trans. Ultrason., Ferroelect., Freq. Contr.*, vol. 43, no. 6, pp. 1171–1179, 1996.
[31] M. Luukkala and P. Meriläinen, "Metal plate testing using airborne ultrasound," *Ultrasonics*, pp. 218–221, 1973.
[32] W. M. D. Wright and D. A. Hutchins, "Air-coupled ultrasonic testing of metals using broadband pulses in through-transmission," *Ultrasonics*, vol. 37, pp. 19–22, 1999.
[33] C. M. Fortunko, M. C. Renken, and A. Murray, "Examination of objects made of wood using air-coupled ultrasound," in *Proc. IEEE Ultrason. Symp.*, 1990, pp. 1099–1103.
[34] Z. E. A. Fellah, C. Depolier, and M. Fellah, "Application of fractional calculus to the sound waves propagation in rigid porous materials: Validation via ultrasonic measurements," *Acust. Acta Acust.*, vol. 88, pp. 34–39, 2002.
[35] T. E. Gómez Álvarez-Arenas, L. Elvira, and E. Riera, "Generation of the slow wave to characterize air-filled porous fabrics," *J. Appl. Phys.*, vol. 78, no. 4, pp. 2843–2845, 1995.
[36] L. Kelders, W. Lauriks, and J. L. Allard, "Transmission of ultrasonic waves through porous layers of high flow resistivity saturated by air," *IEEE Trans. Ultrason., Ferroelect., Freq. Contr.*, vol. 46, no. 1, pp. 114–119, 1999.
[37] P. Leclaire, L. Kelders, W. Lauriks, J. F. Allard, and C. Glorieux, "Ultrasonic wave propagation in reticulated foams saturated by different gases: High frequency limit of the classical models," *Appl. Phys. Lett.*, vol. 69, no. 18, pp. 2641–2643, 1996.
[38] A. C. Armand and D. Guyomar, "Caractérisation acoustique et mécanique des aérogels de sílice," *J. Physique III*, vol. 2, no. C1, pp. 759–762, 1992.
[39] T. E. Gómez Álvarez-Arenas, F. Montero, M. Moner-Girona, E. Rodriguez, A. Roig, and E. Molins, "Viscoelasticity of silica aerogels at ultrasonic frequencies," *Appl. Phys. Lett.*, vol. 81, no. 7, pp. 1198–1200, Aug. 2002.
[40] L. Flax, G. C. Gaunaurd, and H. Überall, "Theory of resonance scattering," in *Physical Acoustics*. vol. XV, W. P. Mason and R. N. Thurston, Eds. New York: Academic, 1981.
[41] M. de Billy, "Determination of the resonance spectrum of elastic bodies via the use of short pulses and Fourier transform theory," *J. Acoust. Soc. Amer.*, vol. 79, pp. 219–221, 1986.
[42] C. C. H. Guyott and P. Cawley, "The measurement of through thickness plate vibrations using a pulsed ultrasonic transducer," *J. Acoust. Soc. Amer.*, vol. 83, no. 2, pp. 623–631, 1988.
[43] L. M. Brekhovskikh, *Waves in Layered Media*. New York: Academic, 1960, pp. 61–70.
[44] D. R. Bland, *The Theory of Linear Viscoelasticity*. New York: Pergamon, 1960, pp. 57–115.
[45] R. Truell, C. Elbaum, and B. B. Chick, *Ultrasonic Methods in Solid State Physics*. New York: Academic, 1969, pp. 58–59.
[46] H. J. McSkimin, "Ultrasonic methods for measuring the mechanical properties of liquids and solids," in *Physical Acoustics*. vol. I A, W. P. Mason, Ed. New York: Academic, 1964, pp. 843–846.
[47] T. J. Plona, L. E. Pitts, and W. G. Mayer, "Ultrasonic bounded beam reflection and transmisión effects at a liquid/solid-plate/liquid interface," *J. Acoust. Soc. Amer.*, vol. 59, no. 6, pp. 1324–1328, 1976.
[48] J. M. Claeys and O. Leroy, "Reflection and transmission of bounded sound beams on half-spaces and through plates," *J. Acoust. Soc. Amer.*, vol. 72, no. 2, pp. 585–590, 1982.
[49] M. J. Anderson, P. R. Martin, and C. M. Fortunko, "Resonant transmission of a three-dimensional acoustic sound beam through a solid plate in air: theory and measurement," *J. Acoust. Soc. Amer.*, vol. 98, no. 5, pp. 2628–2638, 1995.
[50] A. B. Temsamani, S. Vandenplas, M. L. D. Lumöri, and L. Van Biesen, "Experimental validation for the diffraction effect in the ultrasonic field of piston transducers and its influence on absorption and dispersión measurements," *IEEE Trans. Ultrason., Ferroelect., Freq. Contr.*, vol. 48, no. 2, pp. 547–559, 2001.
[51] R. Bass, "Diffraction effects in the ultrasonic field of a piston source," *J. Acoust. Soc. Amer.*, vol. 30, no. 7, pp. 602–605, 1958.
[52] M. A. Biot, "Theory of propagation of elastic waves in a fluid-saturated porous solid. I. Low frequency range," *J. Acoust. Soc. Amer.*, vol. 28, pp. 168–178, 1956.
[53] ——, "Theory of propagation of elastic waves in a fluid-saturated porous solid. II. Higher frequency range," *J. Acoust. Soc. Amer.*, vol. 28, pp. 179–191, 1956.
[54] K. Wu, Q. Xue, and L. Adler, "Reflection and transmission of elastic waves from a fluid-saturated porous solid boundary," *J. Acoust. Soc. Amer.*, vol. 87, no. 6, pp. 2349–2358, 1990.
[55] S. Feng and D. L. Johnson, "High-frequency acoustic properties of a fluid/porous solid interface," *J. Acoust. Soc. Amer.*, vol. 74, no. 3, pp. 906–914, 1983.
[56] T. E. Gómez and E. Riera, "The generation of the Biot's slow wave at a fluid-porous solid interface. The influence of impedance mismatch," *J. Physique III*, vol. 4, coll. C5, pp. 187–190, 1994.
[57] F. Montero, T. E. Gómez, A. Albareda, R. Pérez, and J. A. Casals, "High sensitivity piezoelectric transducers for NDE airborne applications," in *Proc. IEEE Ultrason. Symp.*, 2000, pp. 1073–1076.
[58] T. E. Gómez Álvarez-Arenas and F. Montero, "Materiales y técnicas para el acoplamiento mecánico óptimo de piezocerámicas al aire," *Bol. Soc. Esp. Cerám. Vidrio*, vol. 41, pp. 16–21, Jan. 2002.
[59] S. Temkin, *Elements of Acoustics*. New York: Wiley, 1981, pp. 105–107.
[60] D. L. Johnson and T. J. Plona, "Acoustic slow wave and the consolidation transition," *J. Acoust. Soc. Amer.*, vol. 72, no. 2, pp. 556–565, 1982.

Tomás E. Gómez Álvarez-Arenas was born in Madrid, Spain, in 1966. He received the M.S. and Ph.D. degrees in physics in 1989 and 1994, respectively, from the Universidad Complutense of Madrid, Spain.

He joined the Spanish Research Council (CSIC), Madrid, in 1989 where he worked in several Spanish and European research projects and contracts about ultrasonic nondestructive testing (NDT), materials characterization and piezoelectric composites. In 1996 he moved to Glasgow, Scotland, and worked at the Centre for Ultrasonic Engineering, University of Strathclyde, Glasgow, in the fields of air-coupled piezoelectric transducers and numerical modeling of acoustic wave propagation in random composites. In 1998 he received a research contract from the Spanish Science and Education Ministry to come back to the CSIC to study ultrasonic wave propagation in suspensions and membrane processes. In 1999 he obtained a position in the scientific staff of the Instituto de Acústica, CSIC. Actual research interest includes: ultrasonic materials characterization, acoustic propagation in porous materials, ultrasonic NDT, air-coupled piezoelectric transducers, and Lamb waves propagation and generation.